In Situ Electron Diffraction and Resistivity Characterization of Solid State Reaction Process in Cu/Al Bilayer Thin Films

EVGENY T. MOISEENKO, ROMAN R. ALTUNIN, and SERGEY M. ZHARKOV

Solid state reaction processes in Cu/Al thin films have been studied using the methods of *in situ* electron diffraction and electrical resistivity measurements. The solid state reaction in the Cu/Al thin films has been found to begin already at 88 °C with the formation of the Al_2Cu phase in the process of thermal heating in vacuum. The phase sequence at the solid state reaction in the films under study has been determined to be the following: $Al_2Cu \rightarrow AlCu \rightarrow Al_4Cu_9$. A model has been suggested for describing the initial formation stage of intermetallic compounds at the solid state reaction in Cu/Al thin films. According to this model, at the initial stage, the intermetallic compounds are formed as separate crystallites at the interface in the Cu/Al thin films. The suggested model can be applied both to the formation of the first phase, Al_2Cu, and to the subsequent phases: AlCu and Al_4Cu_9. For the Al_4Cu_9 phase the temperature coefficient of the electrical resistivity has been determined to be equal to $\alpha_{Al_4Cu_9} = 1.1 \times 10^{-3}$ K^{-1}.

https://doi.org/10.1007/s11661-019-05602-5
© The Minerals, Metals & Materials Society and ASM International 2020

I. INTRODUCTION

AT present, alloys and composite materials based on Al and Cu are being widely used in different areas of microelectronics and energy production. Thus, copper-cladding aluminum is widely applied for energy transmission.[1] The pair "copper–aluminum" has actively been studied for its application in soldered connections of wire bonding in microelectronic devices.[2,3] Copper and aluminum-based alloys have been used as junctions[4] and absorbers[5] in CMOS technology. An opportunity of using copper and aluminum-based materials for nanojoining has also been considered.[6–9] One of the most important issues concerning intermetallic compounds is the sequence of their formation and mechanisms occurring on the interface of the heterogeneous nanolayers. This is important since the formation of intermetallic compounds can result into a considerable change in the physical properties of the materials. Thus, for example, in Reference 10 it is shown that the formation of intermetallic compounds Al_2Cu and Al_4Cu_9 on the interface of Cu/Al during the thermosonic Cu-wire bonding process results in the increasing strength of the copper aluminum compound. In Reference 11 it is established that the Al_4Cu_9 phase makes the biggest contribution into the mechanical strength of the copper–aluminum compound, while the phase Al_2Cu is extremely fragile and brittle at room temperature. As far as the electrical properties are concerned, in References 12 and 13 it is shown that the formation of intermetallic compounds on the interface of Cu/Al results in the increase of the electrical resistivity. According to the phase diagram,[14] in the system Al-Cu the following intermetallic compounds are formed: Al_2Cu, AlCu, Al_3Cu_4, Al_2Cu_3, Al_4Cu_9, $AlCu_3$. According to the model of the effective heat of formation (EHF),[15,16] on the interface of Cu/Al, the Al_2Cu phase is the first to be formed, which was confirmed experimentally.[17–20] According to the calculation results for the effective heat of formation presented in Reference21 the following sequence of phase formation is to be observed on the interface of Cu/Al: $Al_2Cu \rightarrow AlCu \rightarrow Al_3Cu_4 \rightarrow Al_2Cu_3 \rightarrow Al_4Cu_9$. However, in various experimental works, the researchers present various sets of phases formed on the interface of Cu/Al.[17,22–24] Besides, in spite of a great number of papers devoted to the processes of solid state reactions in Cu/Al thin films, for example,[17–19,24] the initiation temperature of the solid state reaction in the system Cu/Al has not been determined exactly. Different studies give different temperatures: 110 °C,[18,19] 120 °C,[24] 130 °C,[20] 145 °C[25] and 163 °C.[26] It is worth noting that most investigations have been carried out using *ex situ* techniques; which does not allow the authors to determine the exact initiation temperature of the solid state

EVGENY T. MOISEENKO and ROMAN R. ALTUNIN are with the Siberian Federal University, 79 Svobodny pr., Krasnoyarsk, Russia 660041. SERGEY M. ZHARKOV is with the Siberian Federal University and also with the Kirensky Institute of Physics, Federal Research Center KSC SB RAS, Akademgorodok 50/38, Krasnoyarsk, Russia 660036. Contact e-mail: zharkov@iph.krasn.ru.
Manuscript submitted July 20, 2019.
Article published online January 6, 2020

reaction and complete sequence of the formation of intermetallic compounds on the interface between the nanolayers of Cu and Al.

The goal of the present investigation is to establish the initiation temperature of the solid state reaction and phase formation sequence in Cu/Al bilayer thin films using a combination of *in situ* electron diffraction (ED) and resistivity measurement methods.

II. MATERIALS AND METHODS

Cu/Al bilayer thin films were obtained by the method of electron beam evaporation by the successive deposition of the first layer—Cu and second layer—Al onto a substrate using a high vacuum-coating system Bal-Tec MED-020 (the base pressure being 4×10^{-5} Pa). The deposition rate of Cu and Al was about 2 to 3 Å/s. For the deposition materials of high purity grade (ADVENT[27]) were used: Al—99.999 pct, Cu—99.99 pct. As the substrate, fresh-cleaved single crystals of NaCl(001) with the size of 10 × 10 mm and glass with the size of 20 × 20 mm were used. The substrate temperature during the deposition was equal to room temperature. The sequence (substrate/Cu layer/Al layer) was chosen to exclude any contact between the Al layer and NaCl with the aim to minimize the possibility of oxidation for the Al layer

The thickness of the deposited layers was controlled directly during the deposition process using a quartz crystal thickness monitor Bal-Tec QSG 100. The accuracy of the integrated thickness measurement in the case of depositing a material with the known density was better than 1 pct. The thickness of the Cu layer was ≈ 32 nm, Al ≈ 30 nm. During the sample preparation the upper Al layer with the thickness of ≈ 10 nm appeared to be oxidized and further it did not participate in the solid state reaction between the Cu and Al nanolayers. As a result, the thicknesses of the Cu nanolayer and unoxidized Al nanolayer corresponded to the atomic ratio Cu:Al ≈ 9:4.

The investigations of the microstructure, phase and elemental composition of the Cu/Al films were carried out using the methods of transmission electron microscopy (TEM), electron diffraction and energy-dispersive spectroscopy (EDS) using a high-resolution transmission electron microscope JEOL JEM-2100, equipped with the energy-dispersive spectrometer Oxford Inca x-sight.

To investigate the process of the solid state reaction the Cu/Al films were heated directly in the column of the transmission electron microscope JEOL JEM-2100 using a sample holder with the possibility of controlled heating from room temperature to + 1000 °C (Gatan Model 652 Double Tilt Heating Holder). Simultaneously, with the heating, electron diffraction patterns were registered and the temperature of the samples was measured. The electron diffraction patterns were interpreted using the software DigitalMicrograph (Gatan) and the databases of crystal structures—ICDD PDF 4+[28] and Pearson's Crystal Data.[29] The phase content was quantitatively analyzed using the software for processing electron diffraction patterns—Process Diffraction.[30,31]

This above-mentioned method was successfully used by the authors for the research of structural phase transformations occurring in the solid state reaction process in various thin film nanosystems: Cu/Au,[32] Al/Pt,[33] Fe/Pd,[32,34,35] Fe/Si,[36] Fe-ZrO_2,[37] Co-ZrO_2,[38] Co-In_2O_3.[39]

In order to carry out *in situ* experiments with heating in the transmission electron microscope, the samples deposited on NaCl, immediately after the deposition, were separated from the substrate by submerging them into aquabidest for several seconds, then the films rose to the surface and were placed onto a molybdenum TEM support grid, with the remaining water being immediately removed with filter paper. The absence of defects (exfoliation) in the films after placing them onto the grid was controlled with an optical microscope Nikon Eclipse LV 100. Then, the grid with the sample was fixed in the TEM holder for heating and placed into the column of the transmission electron microscope JEOL JEM-2100 (the vacuum being 1.0×10^{-5} Pa). In the case of the given film preparation technique, the film was in contact with atmosphere and water for as little time as possible which enabled one minimize the formation of an oxide layer on the surface of Al and to obtain reproducible results.

The measurement of the changes in the electrical resistivity of the obtained samples in the process of their heating in high vacuum (10^{-4} Pa) was carried out by the four probe method. The research was done using the films placed on a glass substrate. The simultaneous measurement of the sample temperature and electrical resistivity was made using a unit consisting of a Keithley 2450 SourceMeter and a Keithley DMM6500 digital multimeter.

III. RESULTS AND DISCUSSION

The analysis of a transmission electron microscopy image (Figure 1(a)) and electron diffraction pattern (Figure 1(b)), obtained from the Cu/Al films in the initial state shows that the Cu/Al films consist of Cu crystallites (PDF card #00-004-0836, the space group Fm-3m, lattice constant a = 3.615 Å) and Al (PDF card #00-004-0787, the space group Fm-3m, lattice constant a = 4.049 Å), with the size of 10 to 20 nm. In the electron diffraction patterns obtained from the samples, a complete set of diffraction reflections of the polycrystalline type is observed which is characteristic of the above-mentioned face-centered cubic phases of Cu and Al.

The analysis of the energy-dispersive spectrum (Figure 2) showed that at the initial state the Cu/Al film contained the following elements: Cu, Al, O. Table I presents the normalized values of the elemental content. After heating the film to 600 °C the elemental content did not undergo any changes, which evidenced the fact that oxygen in the initial state was in the bound state but not in the adsorbed one.

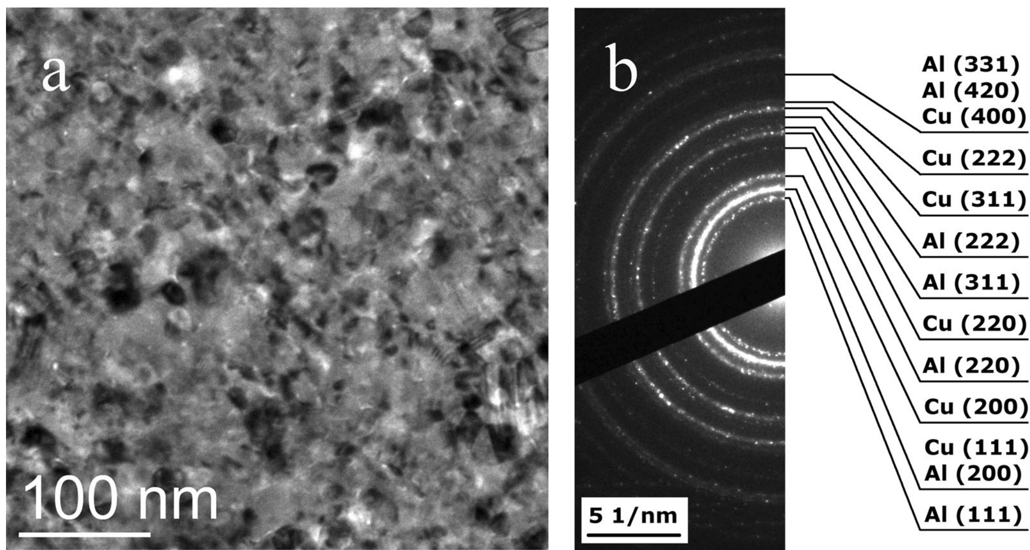

Fig. 1—TEM image (*a*) and electron diffraction pattern (*b*), obtained from the Cu/Al film at the initial state.

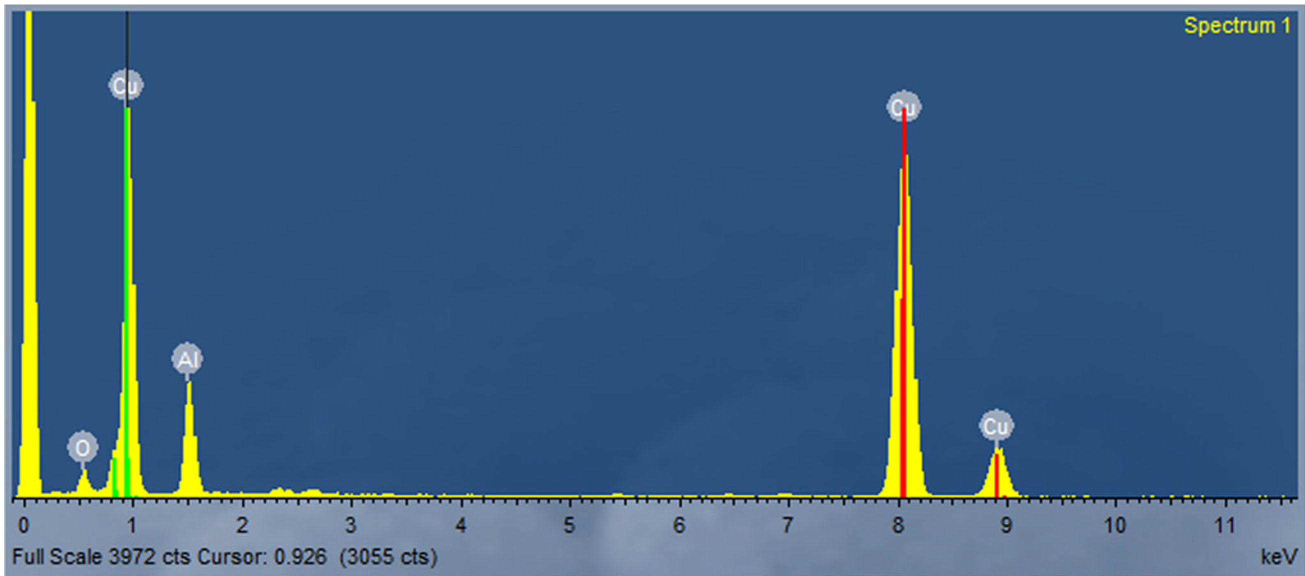

Fig. 2—EDS spectrum obtained from the Cu/Al film at the initial state.

Table I. The Elemental Content of the Cu/Al Films (Atomic Percent)

Spectrum	Cu	Al	O	Total
1	51.4	33.2	15.4	100

It is known that as a result of the interaction with atmospheric air and water, there occurs oxidation of the upper Al layer, with the formation of an amorphous aluminum oxide Al_2O_3, its the minimum thickness being 1 to 10 nm.[40,41] The research of the elemental content of Cu/Al shows that in the initial condition the films contained oxygen ≈ 15.4 at. pct. Assuming that all the oxygen observed belongs to the Al_2O_3 phase and taking into account that the thickness of the Al layer was ≈ 30 nm it is possible to estimate the layer of the oxidized aluminum. The thickness of the oxidized aluminum upper layer obtained as a result of such estimation amounts to ≈ 9.3 nm. Since the oxidized aluminum, as a result of this process, becomes unreactive and further does not participate in the solid state reaction between the Cu and Al nanolayers, then, the effective ratio of copper and aluminum which participate in the solid sate reaction is: Cu:Al ≈ 51.4:22.9 ≈ 2.24, this being very close to the ratio in the compound Al_4Cu_9 (Cu:Al = 2.25).

It is worth noting that in the electron diffraction pattern (see Figure 1(b)), of the Cu/Al film in the initial state no reflections characteristic for Al_2O_3 are observed. However, taking into account the thickness

of the formed Al_2O_3 layer of ($\approx$ 9.3 nm), as well as the fact that it is an amorphous,[40] one can claim that the expected intensity of the diffraction reflections of Al_2O_3 will be at the background level which will be impossible to detect.

To study the solid state reaction process in the system Cu/Al, the obtained bilayer films were heated from room temperature to 600 °C at a rate of 4 °C/min. Simultaneously with the heating, electron diffraction patterns were registered at a rate of 4 frames/min. Thus, the electron diffraction patterns were acquired with the temperature resolution of 1 frame/°C. Then, as a result of processing the electron diffraction patterns, the intensity profiles of the diffraction reflections were obtained for different temperatures (see Figure 3).

For this purpose, with the help of the software package CrystBox[42] the coordinates of the centers of the electron diffraction patterns were determined. Then, using the obtained coordinates, with the help of the software package Gatan DigitalMicrograph, the intensity profiles of the electron diffraction patterns were obtained. Further, with the help of the software package Process Diffraction,[30,31] the background subtraction from the intensity profiles was carried out, with the background being subtracted uniformly for all the intensity profiles obtained, which allowed one to standardize the values of the intensity profiles of the reflections. In the numerical processing of the intensity profiles obtained in such a way, use was made of the software package Process Diffraction,[30,31] which allowed estimating the volumetric content of the phases in the films under study.

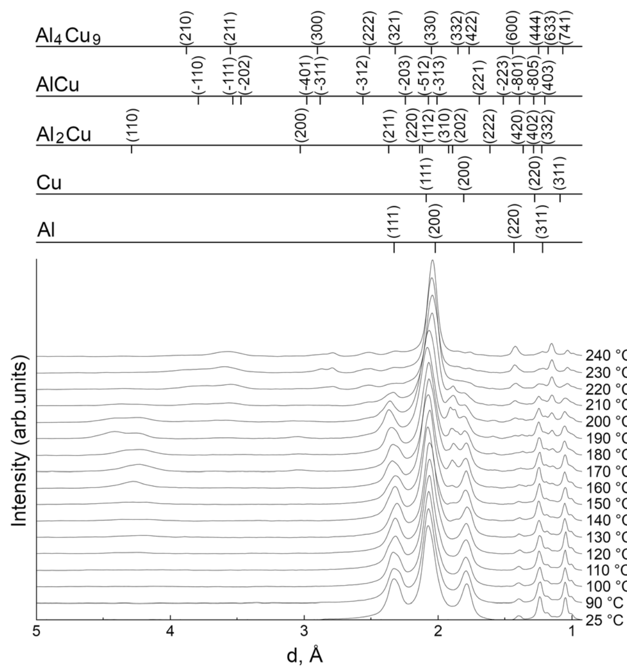

Fig. 3—The intensity profiles of the diffraction reflections in the electron diffraction patterns obtained from the Cu/Al film in the process of heating at a rate of 4 °C/min.

In the upper part of Figure 3, one can see the positions of the reflections characteristic of the phases observed in this work.

Based on the analysis of the intensity profiles of the diffraction reflections, it is possible to plot the dependence of the change in the volumetric content of the observed intermetallic phases in the Cu/Al film in the process of the solid state reaction initiated by heating (see Figure 4).

The analysis of the obtained dependences (see Figure 4) shows that the solid state reaction between the aluminum and copper nanolayers begins at a temperature of $\approx$ 88 °C with the formation of the phase Al_2Cu (PDF card #00-025-0012, the space group I4/mcm, lattice constants: $a = b = 6.065$ Å, $c = 4.873$ Å). At this temperature, the first changes are indicated (Figure 5(a)) in the electron diffraction patterns obtained from the samples in the process of heating, namely the appearance of several diffraction spots with a low intensity corresponding to the interplanar distances $d(200) = 3.03$ Å, $d(202) = 1.90$ Å and $d(310) = 1.92$ Å of the phase Al_2Cu. As a result of the analysis of the observed reflections, it is established that they were obtained from several separate crystallites with the size of 5 to 10 nm. In the course of further heating, the growth of Al_2Cu crystallites was observed, which was evidenced by the increase of the number and intensity of the diffraction reflections in the electron diffraction pattern (see Figure 5(b)).

It is worth noting that in this work, the initiation temperature of the solid state reaction in the Cu/Al films was determined by the analysis of the changes in the electron diffraction patterns obtained in the process of heating, while in many other papers the following methods were used: differential scanning calorimetry,[17] *in situ* X-ray structure analysis,[20,24,26] *in situ* Rutherford backscattering (RBS) analysis,[26] and *ex situ* atom probe tomography.[18,19]

In Reference 24 the investigation was carried out on bilayer films with different Cu/Al thickness ratios which corresponded to different compositions (29, 44, 50, 55,

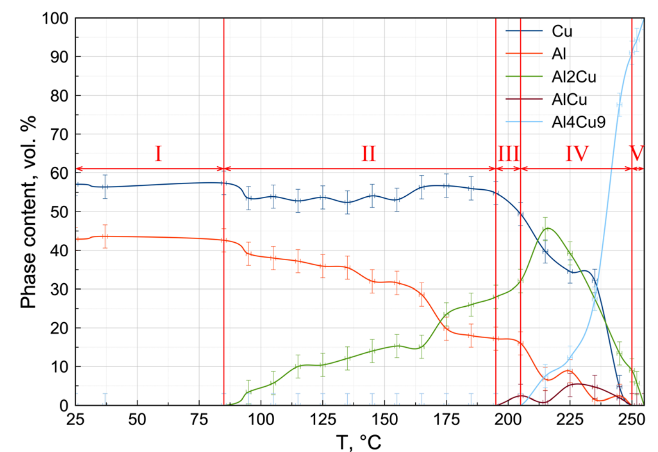

Fig. 4—The dependence of the volumetric content of the phases Cu, Al, Al_2Cu, AlCu, Al_4Cu_9 on the temperature in the process of heating the Cu/Al film.

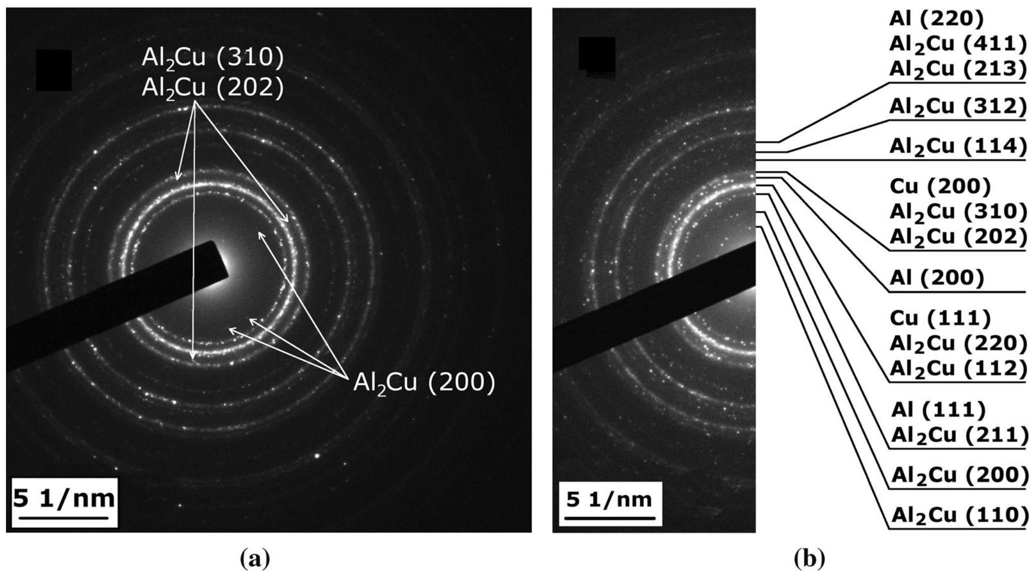

Fig. 5—Electron diffraction patterns, obtained from the Cu/Al film after heating to 88 °C (*a*) and 170 °C (*b*).

60, 64, 69 and 77 at. pct Cu). For all the samples, the total film thickness was 120 nm. For *in situ* X-ray diffraction (XRD) measurements, the samples were loaded into an XRD chamber, equipped with a heating stage in a vacuum of about 10^{-3} Pa. The XRD measurements were performed each 10 °C from 50 °C to 400 °C. The heating rate between the XRD measurements was 5 °C/min. Irrespectively of the atomic composition, the first phase appears at about 120 °C, and it corresponds to Al_2Cu.

In Reference 20, the first nucleating compound (Al_2Cu) was detected at temperatures as low as 130 °C by the XRD analysis during *in situ* annealing in the temperature range 35 °C to 500 °C. The investigation was conducted on a Cu/Al bilayer film. The Cu:A1 atomic ratios of the thin film couples varied from 5:1 to 1:2 with the total thickness not exceeding 700 nm. And the same authors in Reference 26 inform about the formation of a Al_2Cu phase during the annealing of a Cu(90 nm)/Al (160 nm) bilayer film at 163 °C. A quantitative study was carried out using *in situ* RBS.

In Reference 18 and 19 it is shown that the reaction in Al/Cu/Al and Cu/Al/Cu triple layers with an approximately 10-nm single-layer thickness begins after 5 min of annealing at 110 °C with the formation of the Al_2Cu phase. The early stages of reactive interdiffusion were analyzed by means of the atom probe tomography.

It should be noted that in all the above-mentioned investigations[17–20,24,26] the initiation temperature of the solid state reaction in the Cu/Al films detected by different techniques was substantially higher than in the present investigation. This fact could not be explained by the difference in the thicknesses of individual Cu or Al layers, because in some cases, the thickness was several times lower and in some cases, higher, than in the present investigation. The difference in the conditions of the solid state reaction initiation—the heating rate of 5 °C/min in Reference 24 or annealing at a fixed temperature in References 18 and 19, in comparison with the heating rate of 4 °C/min in the present study, also could not be a reason to the considerable increase in the initiation temperature. In addition, the main reasons to explain the difference in the detected temperature of the early stages of the solid state reaction in Cu/Al are the methods which were used to study the reaction and the experimental conditions of conducting the investigations.

All experimental methods have a detection threshold to recognize the presence of a new phase in a sample. According to Reference 26, the minimal effective thickness of the layer to recognize the Al_2Cu phase is ≈ 12 nm for XRD and ≈ 20 nm for RBS analysis. In the case of the electron diffraction method, the minimal effective thickness of a layer can be estimated to ≈ 1 nm. Thus, a phase, smaller in amount than the detection limit, can grow undetected at the interface until its thickness reaches the detection limit. In the case of the atom probe tomography the detection limit is near the atomic monolayer, but it is an *ex situ* method. The minimal temperature used in References 18 and 19 for the annealing of Al/Cu/Al and Cu/Al/Cu triple layers was 110 °C, this is the main reason why they did not observe a lower initiation temperature of the solid state reaction in the Cu/Al system.

In the course of further heating of the Cu/Al thin films at 197 °C, the formation of the phase AlCu begins (PDF card #00-026-0016, the space group C2/m, lattice constants: a = 12.066 Å, b = 4.105 Å, c = 6.913 Å). In this case, it is necessary to note that in the electron diffraction pattern (Figure 6) one can observe only several diffraction spots with a very low intensity $d(001)$ = 5.66 Å and $d(-110)$ = 3.79 Å of the AlCu phase, which allows one to exactly indicate its presence. However, the numerical processing of the electron diffraction patterns and intensity profiles using a special software package Process Diffraction[30,31] made it possible to quantitatively estimate the content of the AlCu phase in spite of the low intensity of the reflections

from this phase. It is worth noting that the maximum content of the AlCu phase in the sample during the solid state reaction did not exceed 5 vol. pct (see Figure 4).

When the temperature of 205 °C is reached, the formation of the phase Al_4Cu_9 begins (PDF card #01–074–7041, the space group P43-m, lattice constant a = 8.685 Å). In the electron diffraction patterns obtained from the sample at the initial stage of the formation of the Al_4Cu_9 phase it was possible to observe only several diffraction spots $d(210)$ = 3.89 Å with very low intensity (see Figure 7(a)), which enables one to exactly identify the presence of the Al_4Cu_9 phase in the sample. As in the case with the AlCu phase, the quantitative estimates of the content of the Al_4Cu_9 phase were obtained as a result of the numerical processing of the obtained electron diffraction patterns and intensity profiles.

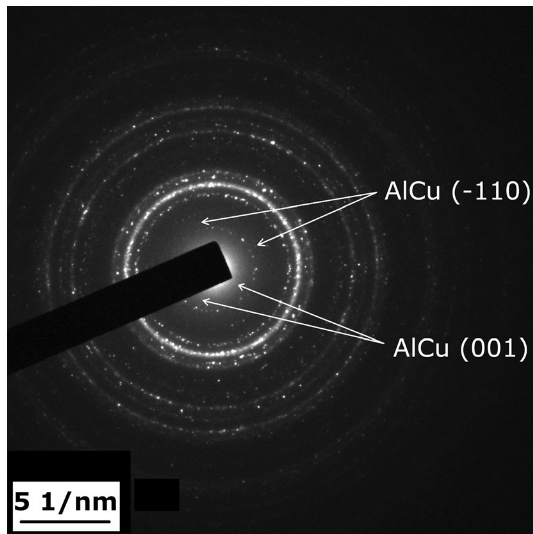

Fig. 6—Electron diffraction patterns, obtained from the Cu/Al film after heating to 197 °C.

In the course of further heating at a temperature of 212 °C, the content of the phases Al_2Cu and AlCu in the sample begins to decrease (see Figure 4). Here, the volumetric content of the Al_4Cu_9 phase increases up to the temperature of 255 °C, at which the Al_4Cu_9 phase is formed in the whole volume of the sample. Upon further heating of the sample to a temperature as high as 600 °C, no changes of the phase composition are observed (see Figure 7(b)).

Based on the results of the analysis of the changes in the content of the phases in the Cu/Al film (the atomic ratio Cu:Al = 9:4) in the process of heating at a rate of 4 °C/min the following sequence of phase formation can be proposed:

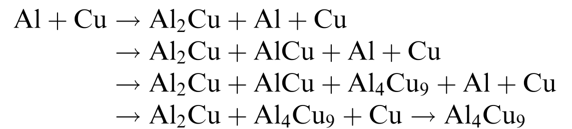

$$\begin{aligned} Al + Cu &\rightarrow Al_2Cu + Al + Cu \\ &\rightarrow Al_2Cu + AlCu + Al + Cu \\ &\rightarrow Al_2Cu + AlCu + Al_4Cu_9 + Al + Cu \\ &\rightarrow Al_2Cu + Al_4Cu_9 + Cu \rightarrow Al_4Cu_9 \end{aligned}$$

Table II presents the sequence for the phases formed in the solid state reaction process in the Cu/Al bilayer thin film nanosystem. It is possible to distinguish six temperature ranges corresponding to different stages of phase formation in the process of the solid state reaction. The first five ranges are shown in Figure 4 and denoted by the Roman numerals.

A phase sequence similar to the one obtained in the present study was obtained in References 43 and 44 According to the phase diagram,[14,45] in the Cu-Al system in the temperature range of 25 °C to 600 °C the formation of the following phases is possible: Al_2Cu, AlCu, Al_3Cu_4, Al_2Cu_3, Al_4Cu_9, $AlCu_4$. According to the EHF model, phases in the process of a solid state reaction are formed in the order of increasing the effective heat of formation.[15,16] For the Cu-Al system, the values of the effective heat of the phase formation

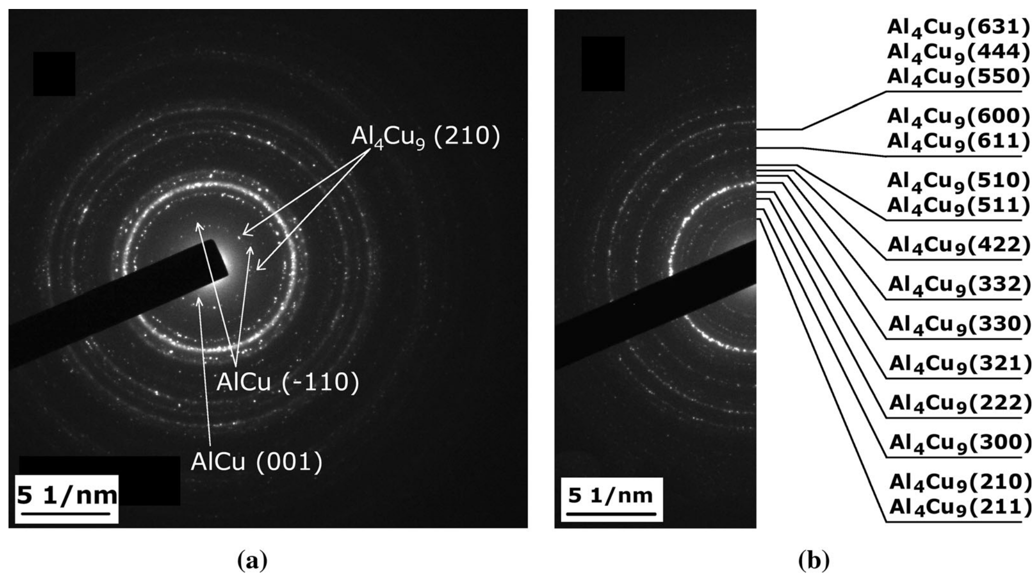

Fig. 7—Electron diffraction patterns, obtained from the Cu/Al film after heating to 205 °C (*a*) and 600 °C (*b*).

Table II. The Sequence of the Phase Formation in the Solid State Reaction Process in the Cu/Al Thin Films

Phase	Temperature, °C 25 to 87 (Range I)	88 to 196 (Range II)	197 to 204 (Range III)	205 to 246 (Range IV)	247 to 254 (Range V)	255 to 600 (Range VI)
Cu	+	+	+	+	+	–
Al	+	+	+	+	–	–
Al_2Cu	–	+	+	+	+	–
AlCu	–	–	+	+	–	–
Al_4Cu_9	–	–	–	+	+	+

$\Delta H'$ are the following: Al_2Cu (– 6.76 kJ/mol); AlCu (– 6.68 kJ/mol); Al_3Cu_4 (– 6.29 kJ/mol); Al_2Cu_3 (– 5.84 kJ/mol); Al_4Cu_9 (– 5.61 kJ/mol).[21] The effective heat of formation of the $AlCu_4$ phase was calculated using the data from Reference 45 and was equal to $\Delta H'_{AlCu_4} = -3.26$ kJ/mol. Thus, according to the EHF model, the sequence of the phase formation in the Cu-Al system has the following form:

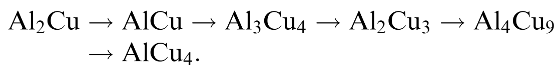

$$Al_2Cu \rightarrow AlCu \rightarrow Al_3Cu_4 \rightarrow Al_2Cu_3 \rightarrow Al_4Cu_9 \rightarrow AlCu_4.$$

It should be noted that the formation of the phases Al_3Cu_4 and Al_2Cu_3 is not observed in the present work, which can be explained by the kinetics of the solid state reaction. In References 46–48, it is shown that rapid diffusion along the grain boundaries at a solid state reaction in thin films will lead to a lower nucleation rate of some phases at the interface or to the complete nucleation suppression of these phases. This also explains why the AlCu phase is formed in small amounts in the process of the solid state reaction between the copper and aluminum layers. The final phase observed in the present study (Al_4Cu_9) is different from the one predicted by the EHF model since the initial effective atomic ratio in the Cu/Al films corresponded to the Al_4Cu_9 phase.

For establishing the relationship between the changes in the phase content studied by the method of *in situ* electron diffraction and the electrical properties, measurements were made of the change in the value of the electrical resistivity ρ of the Cu/Al film in the solid state reaction process. The electrical resistivity was measured on the Cu/Al films deposited on a glass substrate in the process of their heating in high vacuum (4×10^{-5} Pa).

Figure 8 presents the dependence of the value of the electrical resistivity ρ of the Cu/Al film on the temperature of heating in the process of the solid state reaction initiated by this heating between the copper and aluminum nanolayers. One should note that the electrical conductivity value of the Cu/Al film in the initial state, ρ = 7.76 $\mu\Omega$ cm, is considerably higher than those for copper and aluminum (ρ_{Cu} = 1.68 $\mu\Omega$ cm, ρ_{Al} = 2.50 $\mu\Omega$ cm for bulk materials[49]), which is explained by the small size of crystallites in the initial state (10 to 20 nm) and a big amount of intergranular boundaries. In the plot (see Figure 8) several areas can

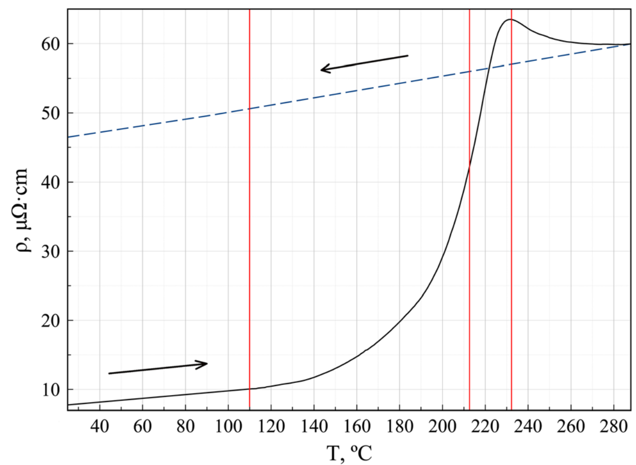

Fig. 8—The dependence of the value of electrical resistivity ρ of the Cu/Al film on the heating temperature.

be distinguished. Thus, from room temperature to 110 °C the increase of the electrical resistivity of the film can be explained by the temperature coefficient of electrical resistivity (4.6×10^{-3} K^{-1} for aluminum and 4.4×10^{-3} K^{-1} for copper[49]). At 110 °C, the electrical resistivity is found to increase, which is due to the formation of the Al_2Cu phase in the process of the solid state reaction. One should pay attention to the fact that the initiation temperature of the solid state reaction in the Cu/Al films estimated taking into account the change in the electrical resistivity is higher than that determined based on the analysis of the electron diffraction patterns (88 °C, see Figure 5(a) and Table II). This can be explained by the following model for the initial stage of formation of intermetallic compounds at the solid state reaction in the Cu/Al thin films. The solid state reaction begins with the formation of the Al_2Cu phase at the interface in the form of several discrete crystallites which do not considerably influence the electrical resistivity of the whole film. During the formation of a considerable amount of crystallites of the new phase, the integral resistivity of the film begins to increase since the resistivity of the Al_2Cu phase (ρ_{Al2Cu} = 8 $\mu\Omega$ cm for bulk material[25]) is considerably higher than the resistivity of the initial materials (ρ_{Cu} = 1.68 $\mu\Omega$ cm, ρ_{Al} = 2.50 $\mu\Omega$ cm[49] for bulk materials). In the course of heating in the range

110 °C to 212 °C the electrical resistivity of the Cu/Al film is observed to increase, this increase being almost parabolic, which is caused by the growth of the Al_2Cu phase. Upon reaching the temperature of 212 °C the growth rate of this value becomes linear which can be due to the beginning formation of the Al_4Cu_9 phase. As it is shown above (see Figure 7(a) and Table II), the Al_4Cu_9 phase begins to form at 205 °C. Thus, it can be claimed that at the initial stages the formation of the Al_4Cu_9 phase goes according to the same model as Al_2Cu, which explains the temperature difference for the beginning of the formation of this phase determined by the analysis of the electron diffraction patterns and temperature dependence of the electrical resistivity. As far as the AlCu, phase is concerned, assuming that its formation occurs according to the above-mentioned model and taking into account that its content in the films under study does not exceed 5 vol. pct (see Figure 4), it can be stated that its formation has no significant influence on the integral electrical resistivity of the films under study. At 215 °C the content of the Al_2Cu phase in the films begins to decrease (see Figure 4), thus, further increase in the electrical resistivity at heating to 232 °C is caused by the growth of the Al_4Cu_9 phase ($\rho_{Al_4Cu_9} = 14.2\ \mu\Omega$ cm in the case of bulk materials[25]). In the temperature range 232 °C to 288 °C, the decrease in the electrical resistivity value is observed, which is explained by the increasing crystallites size of the Al_4Cu_9 phase. The analysis of the electron diffraction patterns and electron microscopy images shows that in the temperature range of 205 °C to 288 °C the crystallite size of the Al_4Cu_9 phase increases from 5 to 10 nm to 20 to 30 nm.

The research of the changes in the electrical resistivity of the film in the process of cooling from 288 °C to room temperature was also carried out (see Figure 8). As a result of the obtained dependence, the temperature coefficient of the electrical resistivity for the phase Al_4Cu_9 was calculated to be $\alpha = 1.1 \times 10^{-3}\ K^{-1}$. The obtained estimate of temperature coefficient of the electrical resistivity corresponds to the values obtained for the Al_4Cu_9 phase in the bulk samples (α = 3.64 to $3.71 \times 10^{-3}\ K^{-1}$[50]) and films with the thickness from 500 nm ($\alpha = 3.64 \times 10^{-3}\ K^{-1}$[50]) to 3.5 μm ($\alpha = 1.64 \times 10^{-3}\ K^{-1}$[51]).

It is worth noting that the final electrical resistivity value of the Al_4Cu_9 phase at room temperature obtained in the present study, $\rho_{Al_4Cu_9} = 46.48\ \mu\Omega$ cm is considerably higher than the electrical resistivity of this phase in the bulk state ($\rho_{Al_4Cu_9} = 14.2\ \mu\Omega$ cm[25]). The authors of[24] present the temperature dependences of the electrical resistivity for the Cu/Al thin film system (the atomic ratio Cu:Al $\approx$ 9:4) in the solid state reaction process upon heating in the range from room temperature to 400 °C. The character of the temperature dependence of the electrical resistivity in Reference 24 is similar to the results obtained in the present study. Besides, the electrical resistivity value of the Al_4Cu_9 phase obtained in Reference 24 ($\rho_{Al_4Cu_9} = 53\ \mu\Omega$ cm), is close to the result obtained in this work ($\rho_{Al_4Cu_9} = 46.48\ \mu\Omega$ cm). It can be assumed that the high electrical resistivity values of the phases obtained as a result of the solid state reactions in thin films are due to the small crystallite size (in the present study it is equal to 20 to 30 nm) and a big number of intergranular boundaries. The electrical resistivity is known to increase considerably with the decrease of the crystallite size.[52]

IV. CONCLUSIONS

The methods of *in situ* electron diffraction allowed one to establish that a solid state reaction in Cu/Al thin films began already at 88 °C with the formation of the Al_2Cu phase in the process of thermal heating in vacuum. At 197 °C the AlCu phase began to form. The final phase is Al_4Cu_9, the beginning of its formation was observed at 205 °C. The phase sequence at the solid state reaction in the films under study was determined to be the following: $Al_2Cu \rightarrow AlCu \rightarrow Al_4Cu_9$. From the analysis of the results obtained using the methods of *in situ* electron diffraction and electric resistivity measurements a model was suggested for describing the initial formation stage of intermetallic compounds at the solid state reaction in Cu/Al thin films. According to this model, at the initial stage, the intermetallic compounds are formed as separate crystallites at the interface in the Cu/Al thin films. The suggested model can be applied both to the formation of the first phase, Al_2Cu, and to the subsequent phases: AlCu and Al_4Cu_9. For the Al_4Cu_9 phase in the thin films, the temperature coefficient of the electrical resistivity was determined to be equal to $\alpha_{Al_4Cu_9} = 1.1 \times 10^{-3}\ K^{-1}$.

ACKNOWLEDGMENTS

The authors wish to thank the financial support from the Russian Science Foundation (Grant #18-13-00080).

REFERENCES

1. D. Chu, J.-Y. Zhang, J.-J. Yao, Y.-Q. Han, and C.-J. Wu: *Trans. Nonferr. Met. Soc. China*, 2017, vol. 27, pp. 2521–28, https://doi.org/10.1016/S1003-6326(17)60279-6.
2. H. Xu, C. Liu, V.V. Silberschmidt, S.S. Pramana, T.J. White, and Z. Chen: *Scr. Mater*., 2009, vol. 61, pp. 165–68, https://doi.org/10.1016/j.scriptamat.2009.03.034.
3. C.J. Hang, C.Q. Wang, M. Mayer, Y.H. Tian, Y. Zhou, and H.H. Wang: *Microelectron. Reliab*., 2008, vol. 48, pp. 416–24, https://doi.org/10.1016/j.microrel.2007.06.008.
4. A.I. Oliva, J.E. Corona, and V. Sosa: *Mater. Charact*., 2010, vol. 61, pp. 696–702, https://doi.org/10.1016/j.matchar.2010.03.016.
5. M.R.S. Dias, C. Gong, Z.A. Benson, and M.S. Leite: *Adv. Opt. Mater*., 2018, vol. 6, pp. 1700830–8, https://doi.org/10.1002/adom.201700830.
6. Y.N. Zhou: *Microjoining and nanojoining*, Woodhead Publishing, Cambridge, 2008, ISBN 9781845691790.
7. A.S. Rogachev, S.G. Vadchenko, and A.S. Mukasyan: *Appl. Phys. Lett*., 2012, vol. 101, pp. 063119–4, https://doi.org/10.1063/1.4745201.

8. A.S. Rogachev, S.G. Vadchenko, F. Baras, O. Politano, S. Rouvimov, N.V. Sachkova, M.D. Grapes, T.P. Weihs, and A.S. Mukasyan: *Combust*. *Flame*, 2016, vol. 166, pp. 158–69, https://doi.org/10.1016/j.combustflame.2016.01.014.
9. D.J. Fisher: *Bonding by self-propagating reaction*, Materials Research Forum LLC, Millersville, PA, 2019, ISBN 978-1-64490-008-6.
10. J. Li, L. Liu, L. Deng, B. Ma, F. Wang, and L. Han: *IEEE Electr*. *Device Lett*., 2011, vol. 32, pp. 1433–35, https://doi.org/10.1109/LED.2011.2161749.
11. D. Zuo, S. Hu, J. Shen, and Z. Xue: *Mater*. *Des*., 2014, vol. 58, pp. 357–62, https://doi.org/10.1016/j.matdes.2014.02.004.
12. W.-B. Lee, K.-S. Bang, and S.-B. Jung: *J*. *Alloy*. *Compd*., 2005, vol. 390, pp. 212–19, https://doi.org/10.1016/j.jallcom.2004.07.057.
13. J. Zhang, B.-H. Wang, G.-H. Chen, R.-M. Wang, C.-H. Miao, Z.-X. Zheng, and W.-M. Tang: *Trans*. *Nonferr*. *Met*. *Soc*. *China*, 2016, vol. 26, pp. 3283–91, https://doi.org/10.1016/S1003-6326(16)64462-X.
14. J.L. Murray: *Int*. *Met*. *Rev*., 1985, vol. 30, pp. 211–34, https://doi.org/10.1179/imtr.1985.30.1.211.
15. R. Pretorius, A.M. Vredenberg, F.W. Saris, and R. de Reus: *J*. *Appl*. *Phys*., 1991, vol. 70, pp. 3636–46, https://doi.org/10.1063/1.349211.
16. R. Pretoriuos, Ch.C. Theron, A. Vantomme, and J.W. Mayer: Critical reviews in solid state and materials*Science*, 1999, vol. 24, pp. 1–62, https://doi.org/10.1080/10408439991329161.
17. H.G. Jiang, J.Y. Dai, H.Y. Tong, B.Z. Ding, Q.H. Song, and Z.Q. Hu: *J*. *Appl*. *Phys*., 1993, vol. 74, pp. 6165–69, https://doi.org/10.1063/1.355183.
18. C.B. Ene, G. Schmitz, T. Al-Kassab, and R. Kirchheim: *Ultramicroscopy*, 2007, vol. 107, pp. 802–07, https://doi.org/10.1016/j.ultramic.2007.02.012.
19. C.B. Ene, Thermal stability and reaction of metallic multilayers, Dissertation zur Erlangung des Doktorgrades der Mathematisch-Naturwissenschaftlichen Fakultäten der Georg-August-Universität Göttingen, 2007, 120 p. http://hdl.handle.net/11858/00-1735-0000-0006-B464-6.
20. J.M. Vandenberg and R.A. Hamm: *Thin Solid Films*, 1982, vol. 97, pp. 313–23, https://doi.org/10.1016/0040-6090(82)90523-5.
21. Y. Guo, G. Liu, H. Jin, and Z. Shi: *J*. *Mater*. *Sci*., 2011, vol. 46, pp. 2467–73, https://doi.org/10.1007/s10853-010-5093-0.
22. D.L. Zhang and D.Y. Ying: *Mater*. *Sci*. *Eng*. *A*, 2001, vol. 301, pp. 90–96, https://doi.org/10.1016/S0921-5093(00)01388-5.
23. H. Xu, I. Qin, H. Clauberg, B. Chylak, and V.L. Acoff: *Scr*. *Mater*., 2016, vol. 115, pp. 1–5, https://doi.org/10.1016/j.scriptamat.2015.12.025.
24. F. Haidara, M.-C. Record, B. Duployer, and D. Mangelinck: *Surf*. *Coat*. *Techn*., 2012, vol. 206, pp. 3851–56, https://doi.org/10.1016/j.surfcoat.2012.01.065.
25. J.A. Rayne, M.P. Shearer, and C.L. Bauer: *Thin Solid Films*, 1980, vol. 65, pp. 381–90, https://doi.org/10.1016/0040-6090(80)90248-5.
26. R.A. Hamm and J.M. Vandenberg: *J*. *Appl*. *Phys*., 1984, vol. 56, pp. 293–99, https://doi.org/10.1063/1.333960.
27. ADVENT Research Materials Ltd, Oxford, U.K. https://www.advent-rm.com.
28. Powder Diffraction File (PDF 4+, 2018), Inorganic Phases Database, International Center for Diffraction Data (ICDD), Swarthmore, PA. http://www.icdd.com/products/pdf4.htm.
29. P. Villars, K. Cenzual, Pearson's Crystal Data: Crystal Structure Database for Inorganic Compounds (on CD-ROM), Release 2011/12, ASM International®, Materials Park, OH.
30. J.L. Lábár: *Microsc*. *Microanal*., 2008, vol. 14, pp. 287–95, https://doi.org/10.1017/S1431927608080380.
31. J.L. Lábár: *Microsc*. *Microanal*., 2009, vol. 15, pp. 20–29, https://doi.org/10.1017/S1431927609090023.
32. S.M. Zharkov, E.T. Moiseenko, and R.R. Altunin: *J*. *Solid State Chem*., 2019, vol. 269, pp. 36–42, https://doi.org/10.1016/j.jssc.2018.09.009.
33. R.R. Altunin, E.T. Moiseenko, and S.M. Zharkov: *Phys*. *Solid State*, 2018, vol. 60, pp. 1413–18, https://doi.org/10.1134/S106378341807003X.
34. S.M. Zharkov, E.T. Moiseenko, R.R. Altunin, N.S. Nikolaeva, V.S. Zhigalov, and V.G. Myagkov: *JETP Lett*., 2014, vol. 99, pp. 405–09, https://doi.org/10.1134/S0021364014070145.
35. E.T. Moiseenko, R.R. Altunin, and S.M. Zharkov: *Phys*. *Solid State*, 2017, vol. 59, pp. 1233–37, https://doi.org/10.1134/S1063783417060154.
36. S.M. Zharkov, R.R. Altunin, E.T. Moiseenko, G.M. Zeer, S.N. Varnakov, and S.G. Ovchinnikov: *Solid State Phenom*., 2014, vol. 215, pp. 144–49, https://doi.org/10.4028/www.scientific.net/SSP.215.144.
37. V.G. Myagkov, L.E. Bykova, O.A. Bayukov, V.S. Zhigalov, I.A. Tambasov, S.M. Zharkov, A.A. Matsynin, and G.N. Bondarenko: *J*. *Alloys Compd*., 2015, vol. 636, pp. 223–28, https://doi.org/10.1016/j.jallcom.2015.02.012.
38. V.G. Myagkov, V.S. Zhigalov, L.E. Bykova, S.M. Zharkov, A.A. Matsynin, M.N. Volochaev, I.A. Tambasov, and G.N. Bondarenko: *J*. *Alloys Compd*., 2016, vol. 665, pp. 197–203, https://doi.org/10.1016/j.jallcom.2015.12.257.
39. L.E. Bykova, S.M. Zharkov, V.G. Myagkov, V.S. Zhigalov, G.S. Patrin: *JOM*, 2020, vol. 72 (In Press). https://doi.org/10.1007/s11837-019-03919-5.
40. R.W. Revie, H.H. Uhlig: *Corrosion and Corrosion Control*, 4th ed., Wiley, New Jersey, 2008; https://doi.org/10.1002/9780470277270. ISBN 9780470277270. http://onlinelibrary.wiley.com/book/10.1002/9780470277270.
41. R.W. Revie: *Uhlig's Corrosion Handbook*, 3rd ed., Wiley, New Jersey, 2011. ISBN 9780471784944.
42. M. Klinger. *CrysTBox—Crystallographic Toolbox*. Institute of Physics of the Czech Academy of Sciences, 2015. ISBN 978-80-905962-3-8. http://www.fzu.cz/~klinger/crystbox.pdf.
43. H.T.G. Hentzell and K.N. Tu: *J*. *Appl*. *Phys*., 1983, vol. 54, pp. 6929–37, https://doi.org/10.1063/1.332000.
44. H.T.G. Hentzell, R.D. Thompson, and K.N. Tu: *Mater*. *Lett*., 1983, vol. 2, pp. 81–84, https://doi.org/10.1016/0167-577X(83)90041-1.
45. B. Predel, Al-Cu (Aluminum-Copper), in O. Madelung (Ed.), Landolt-Börnstein—Group IV Physical Chemistry, Vol. 5A (Ac-Au—Au-Zr), Springer, Berlin, 1991, Phase Equilibria, Crystallographic and Thermodynamic Data of Binary Alloys. https://doi.org/10.1007/10000866_100. ISBN 978-3-540-15516-4 (Print) 978-3-540-39444-0 (Online). https://materials.springer.com/lb/docs/sm_lbs_978-3-540-39444-0_100.
46. K. Rajan and E.R. Wallach: *J*. *Cryst*. *Growth*, 1980, vol. 49, pp. 297–302, https://doi.org/10.1016/0022-0248(80)90164-5.
47. R.W. Balluffi and J.M. Blakely: *Thin Solid Films*, 1975, vol. 25, pp. 363–292, https://doi.org/10.1016/0040-6090(75)90056-5.
48. V.I. Dybkov: *J*. *Mater*. *Sci*., 1987, vol. 22, pp. 4233–39, https://doi.org/10.1007/BF01132013.
49. W. Martienssen, H. Warlimont: *Springer handbook of condensed matter and materials data*, Springer-Verlag Berlin Heidelberg, 2005, ISBN 978-3-540-30437-1.
50. C. Macchioni, J.A. Rayne, S. Sen, and C.L. Bauer: *Thin Solid Films*, 1981, vol. 81, pp. 71–78, https://doi.org/10.1016/0040-6090(81)90506-X.
51. S. Pfeifer, S. Großmann: *IEEE 58th Holm Conference on Electrical Contacts (Holm)*, 2012. https://doi.org/10.1109/HOLM.2012.6336554.
52. J.L. McCrea, K.T. Aust, G. Palumbo, and U. Erb: *MRS Online Proc*. *Library Arch*., 1999, vol. 581, pp. 461–66, https://doi.org/10.1557/PROC-581-461.

Publisher's Note Springer Nature remains neutral with regard to jurisdictional claims in published maps and institutional affiliations.